

Synthesis and Characterization of Symmetric Cyclooctatetraindoles: Exploring the Potential as Electron-Rich Skeletons with Extended π -Systems

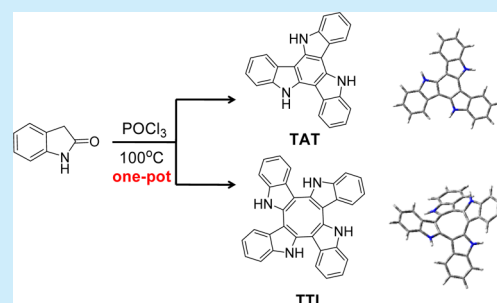
Fang Wang,^{†,§} Xiang-Chun Li,^{†,§} Wen-Yong Lai,^{*,†,‡} Yao Chen,[†] Wei Huang,^{*,†} and Fred Wudl[‡]

[†]Key Laboratory for Organic Electronics & Information Displays (KLOEID), Institute of Advanced Materials (IAM), Nanjing University of Posts and Telecommunications, Nanjing 210023, China

[‡]California NanoSystems Institute (CNSI), University of California, Santa Barbara, California 93106-6105, United States

S Supporting Information

ABSTRACT: A facile one-pot tetramerization of indolin-2-one with phosphoryl chloride was applied for the first convenient direct synthesis of C_{2v} -symmetric cyclooctatetraindole with an 8π annulene as the center. Tetra- and octa-arylated cyclooctatetraindole derivatives functionalized with fluorescent fluorene and pyrene units were thus facily synthesized and characterized.



Indole related molecules are important heteroaromatic compounds in diverse natural products and compounds displaying significant pharmacological and biological activities.¹ They are also being extensively investigated in well-known hole-transporting, light-emitting, and light-harvesting materials and, therefore, are considered as potential building blocks for functional materials due to their excellent electrical and thermal properties.^{2–4} Many indole-based polymers and oligomers have been widely explored. Among them, new indole-related building blocks such as indolo[3,2-*b*]carbazole,³ isoindigo,⁴ and 10,15-dihydro-5*H*-diindolo[3,2-*a*:3',2'-*c*]carbazole (triindole or triazatruxene, TAT) (Figure 1)^{5–8} have attracted much recent interest. This kind of compound constitutes two or three indole units linked together or fused via an extra six-membered benzene ring with extended π -systems. Such novel structures have proven to be very promising platforms and are being widely investigated in the field of organic electronics, i.e. organic light-emitting diodes,⁵ organic solar cells,^{4,6} field-effect transistors,⁴ liquid crystals,⁷ biosensors,⁸ etc.

Polycyclic hydrocarbons with special topologies have been the subject of particular attention.⁹ Cyclooctatetraene (COT) is one of the typical flexible π -conjugated skeletons,¹⁰ which has an 8π annulene possessing an inherently nonplanar saddle-shaped geometry with D_{2d} symmetry. Various sophisticated COT structures fused with phenyl, thiophene, furan, pyrimidine, thiazole, and benzothiophene have been designed and synthesized;¹¹ these COT-based materials have found interesting applications as cavity-size-controlled cage molecules,¹² electro-mechanical actuators,¹³ buckycatchers,¹⁴ and molecular tweezers.¹⁵ To the best of our knowledge, no such COT fused with indole units has been known until recently.¹⁶

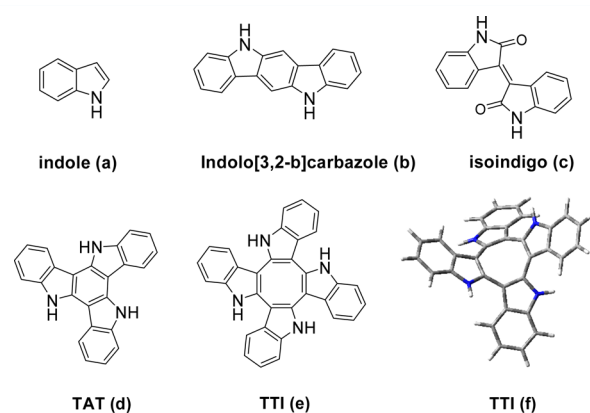


Figure 1. Chemical structures of (a) indole, (b) fused indolo[3,2-*b*]carbazole, (c) isoindigo, (d) triazatruxene or cyclic triindole (TAT), (e) cyclic tetraindole (TTI), and (f) the optimized geometry structure for TTI.

Cyclic indole derivatives, more specifically triindole or triazatruxene (TAT), recently emerged as strong electron-donating and hole-transporting motifs. Recent works by our group and others have established their intriguing potentials as high-performance organic semiconductors for optoelectronics.^{5,6} In contrast, the symmetric cyclic tetramer COT analogue 5,10,15,20-tetrahydrotriindolo[2',3':3,4:2',3':5,6:2',3':7,8]cycloocta[1,2-*b*]indole (tetraindole, TTI) has been very rarely studied, probably due to difficulties in its synthesis.^{17,18} A

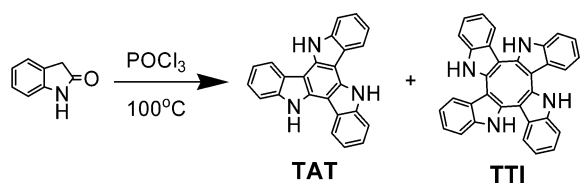
Received: April 15, 2014

theoretical simulation indicates that the cyclic tetraindole rings form a saddle-shaped structure (Figure 1f), with an 8π COT annulene as the center, that could be transformed into an aromatic “planar” form by reduction to a 10π dianion or by oxidation to a 6π dication according to Hückel’s rule. Furthermore, owing to its cyclic electron-rich tetraindole structure and its twisted saddle-like structure, this C_{2v} -symmetric motif may also be interesting as a central skeleton for the construction of novel molecules with extended π -systems.

As part of our continuing efforts and interest in cyclic indole derivatives,⁵ we report herein a facile one-pot procedure for the first direct synthesis of symmetric cyclic tetraindole. Its potential as electron-rich building blocks for constructing extended π -systems has also been investigated.

Synthesis of cyclic tetraindole was carried out in neat POCl_3 under dry conditions using a one-pot process (Scheme 1).

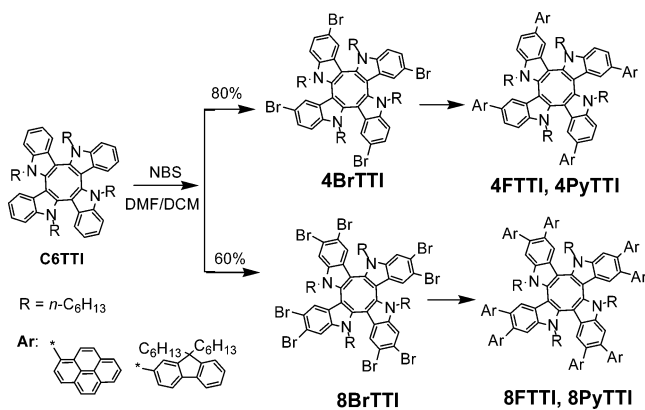
Scheme 1. One-Pot Synthesis toward Symmetric Cyclic Indoles



Unexpectedly, treatment of indolin-2-one in POCl_3 provided triindole and tetraindole mixtures. The isolated yields of the products were varied with different reaction conditions that were found to be significantly dependent upon the added amount of POCl_3 (Table S1). When indolin-2-one (3 g, 14.5 mmol) was treated with phosphoryl chloride (POCl_3 , 20.0 mL) at 100°C for 8 h, **TTI** (16%) and **TAT** (18%) were afforded. Following alkylation with 1-bromohexene in basic conditions, **C6TTI** was afforded in high yield (80%). *N*-Bromosuccinimide (NBS) was found to be successful for the direct bromination of **C6TTI**. Tetra- and octabrominated tetraindoles were then achieved easily by adjusting the molar ratios of NBS.

To investigate the impact of the cyclooctatetraindole core structure on functions of the resulting molecules, the bromo substituents were then replaced by fluorescent fluorene and pyrene units. The synthetic routes to tetra- and octa-arylated tetraindoles, **4FTTI**, **8FTTI**, **4PyTTI**, and **8PyTTI**, are shown in Scheme 2. A well-developed microwave-enhanced multiple coupling strategy was adopted to accelerate the 4- and 8-fold

Scheme 2. Synthetic Routes to Arylated Cyclooctatetraindoles



Suzuki coupling reactions,¹⁹ affording the tetra- and octa-arylated tetraindoles efficiently (21–48%). The resultant starbursts are readily soluble in common solvents, such as CHCl_3 , THF, and toluene.

The structures of the resultant cyclooctatetraindoles were well identified by MALDI-TOF mass spectra, ^1H and ^{13}C NMR spectra, and elemental analysis (Figures S1–S22). The results unequivocally confirmed the symmetrically cyclic nature of **TTI**. MALDI-TOF spectra revealed the molecular ion peak of 461, consistent with that of the indole tetramer. The ^1H NMR of **TTI** shows three signals of aromatic protons (7.56 (d, 4H, $J = 7.6$ Hz), 7.41 (d, 4H, $J = 7.7$ Hz), and 7.09 (dt, 8H, $J = 14.5, 7.0$ Hz) ppm) in CD_3SOCD_3 . These signals indicate a highly symmetrical structure. The successful cyclotetramerization is also evident when comparing the ^1H NMR of **TTI** with those of the starting material indolin-2-one and **TAT** as shown in Figure 2. The NH-

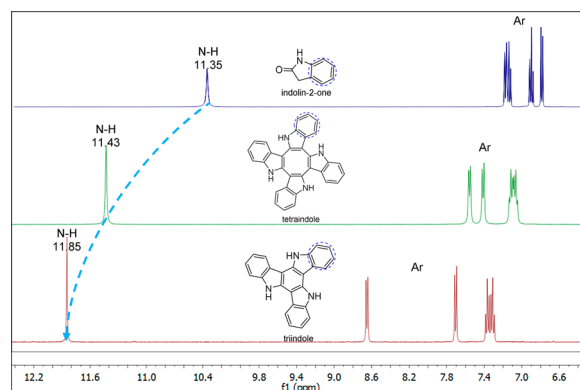


Figure 2. ^1H NMR of **TTI**, **TAT**, and indolin-2-one.

protons for **TTI** appeared at 11.43 (s, 4H) ppm, while the chemical shift of the N–H bond in the ^1H NMR spectra of indolin-2-one and **TAT** appeared at 11.35 and 11.85 ppm, respectively. The existence of the N–H bond in the tetramer according to the ^1H NMR spectra proved the symmetric cyclocondensation of the tetraindole occurred at the 2,3-position of indolin-2-one (Figure 2). Further evidence was also given in the ^{13}C NMR spectrum, in which eight carbon signals were presented at 137.8, 135.2, 127.8, 121.7, 120.0, 119.2, 111.8, and 105.0 ppm. For the reaction with 2,3-couplings of monomeric indole units, only a symmetric cyclotrimer and -tetramer were obtained. Based on the above experimental investigations, the formation of cyclic triindole and tetraindole could probably be elucidated by chlorination of indolin-2-one in the presence of POCl_3 and a further stepwise cyclocondensation mechanism (Scheme S3).

Thermogravimetric analysis revealed that the resultant cyclooctatetraindoles are thermally stable with 5% weight loss temperature up to 360°C for **C6TTI** and over 400°C for the arylated ones (Figure S23, Table 1). No weight loss below 300°C was detected for all the samples, indicative of good thermal stability. Reversible DSC curves were recorded for **C6TTI** with a sharp endothermic peak at 129°C during heating and a sharp exothermic peak at 65°C during cooling (Figure S24), which was ascribed to the melting and crystallization process, respectively. In contrast, no distinctive melting or crystallization transitions were observed during the DSC scans from rt to 250°C for all arylated tetraindoles, suggesting that the resultant starbursts could be amorphous. The amorphous characteristics of the samples were further confirmed by wide-angle X-ray diffraction

Table 1. Thermal and Photophysical Properties of the Cyclooctatetraindoles

	T_d (°C) ^a	$\lambda_{\text{abs,solution}}$ (nm)	ϵ_{max} ($10^4 \text{ L}\cdot\text{mol}^{-1}\cdot\text{cm}^{-1}$) [$\log \epsilon$]	$\lambda_{\text{abs, film}}$ (nm)	$\lambda_{\text{PL,DCM}}$ (nm)	$\lambda_{\text{PL, film}}$ (nm)	λ_{onset} (nm) ^b	E_g^{opt} (eV) ^c
C6TTI	360	312	2.89 [4.46]	321	352	494	410	3.02
4FTTI	412	340	5.10 [4.71]	365	382	466	430	2.88
8FTTI	406	301	3.14 [4.50]	339	368	471	438	2.76
4PyTTI	423	325	4.37 [4.64]	348	508	479	458	2.71
8PyTTI	433	324	3.49 [4.54]	346	558	548	550	2.25

^aTemperature corresponding to 5% weight loss. ^b λ_{onset} was the onset for the film absorption spectra. ^c E_g^{opt} (optical energy gap) calculated from the absorption onset of film spectra.

(WAXD) patterns (Figure S25). The good thermal and morphological stability of these materials enables the preparation of homogeneous and stable amorphous thin films by solution processing, which is crucial for the applications for organic optoelectronics.

The photophysical data of the compounds are collected in Table 1 and Figure S26. For C6TTI, the absorption spectra in dilute DCM solution show an intense π - π^* absorption peak at 312 nm, whereas the absorption spectrum in film (Figure S27) exhibits a strong π - π^* transition at 321 nm with a tail at low energy that might be related to excimers or aggregates of the tetraindole molecules. The emission spectrum of C6TTI is located in the near-ultraviolet region with peak emission at 352 nm, while its thin film displays a large red shift at 494 nm. The arylated tetraindoles exhibit strong π - π^* electron absorption bands, with peaks at 340, 301, 325, and 324 nm, respectively, in dilute DCM solution, whereas their films showed absorption peaks at 365, 339, 348, and 346 nm, respectively. Increasing the *ortho*-substituted fluorene units alongside the tetraindole core structure resulted in significant blue shifts (of 39 and 26 nm) from 340 nm for 4FTTI to 301 nm for 8FTTI in dilute solution and from 365 nm for 4FTTI to 339 nm for 8FTTI in thin films. The results suggest a nonplanar structurally hindered geometry induced by the *ortho* substituents that limit π -delocalization through the tetraindole core. The optical band gaps derived from the absorption edge of film spectra of arylated cyclooctatetraindoles gave values ranging between 2.25 and 2.88 eV, while C6TTI showed a large optical gap of 3.02 eV.

The emission maxima of 4FTTI, 8FTTI, 4PyTTI, and 8PyTTI were recorded at 382, 368, 508, and 558 nm in solution, respectively, whereas they are at 466, 471, 479, and 548 nm, respectively, in films. Significant red shifts in emission spectra were observed for 4FTTI (84 nm) and 8FTTI (103 nm) upon moving from a dilute solution to thin films. To understand the origin of the red-shifted emission, PL spectra with increasing concentration were recorded (Figure S28). Clearly, the resultant arylated tetraindoles exhibited distinct concentration dependent luminescence. With increasing concentration, the long-wavelength emission in the range of 500–600 nm increased progressively. Considering the PL emission peak at 494 nm for C6TTI, such a red-shifted emission could be ascribed to the combination of the radiative decay from the tetraindole core and/or from the molecular aggregates or excimers. According to the absorption spectra of 8PyTTI films in Figure S26d, the aggregate formation was also evident by the appearance of a long-wavelength broad tail ranging from 430 to 550 nm. This red-shifted emission became dominant especially for the pyrene-functionalized tetraindoles at high concentrations probably because of the rigid pyrene structure that tends to form aggregates or excimers in such a crowded structure. Theoretical calculations were performed to further interpret this phenomenon.

The optimized geometries show that the saddle-shaped tetraindole core is significantly twisted, rendering the resultant molecules with a twisted nonplanar structure (Figure 1f). Furthermore, the resultant tetraindoles take a tub conformation with an average bend angle θ of 51.57°, 51.55°, 51.46°, and 51.41°, for 4FTTI, 4PyTTI, 8PyTTI, and 8FTTI, respectively (Scheme S4). These values are a bit smaller than that of TTI ($\theta = 53.12^\circ$). The steric repulsion upon the increase in *ortho*-substituted chromophores may play a role in increasing the planarity of these analogues. These geometrical characteristics are believed to be beneficial to the formation of the amorphous shape for these compounds and, thus, inhibit the molecular crystallization process. This has been evidenced as revealed in thermal and morphology analysis. For 4FTTI, and 8FTTI, an obvious overlap exists between the molecular HOMO and LUMO orbitals (Scheme S6). This overlap indicates that delocalization occurs over the tetraindole core structure. However, for 4PyTTI and 8PyTTI, the LUMO is dominated by the pyrene units for both compounds, while the HOMO is mainly on the tetraindole unit, with little extension to the pyrene segment in 8PyTTI. The HOMO–LUMO energy gaps of the tetraindoles were found to be in the range of 2.83–3.77 eV (B3LYP/6-31G(d), Scheme S6).

The electrochemical characteristics were studied by cyclic voltammetry (CV) to further reveal the electronic properties. The data are collected in Table S2, in comparison with those calculated with B3LYP/6-31G(d). C6TTI exhibited two-electron oxidation processes with a rather low onset oxidation potential (0.32 V), which corresponds to a HOMO value of –5.3 eV. The low onset oxidation potential suggests good electron-donating properties of the resulting tetraindole core, consistent with its electron-rich nature considering the symmetric cyclic tetraindole core structure with four nitrogen bridges. The oxidation process of the C6TTI film was pseudo reversible, whereas the reduction process was essentially irreversible (Figure 3a). Such a redox behavior is reasonable considering the good electron-donating ability for the cyclic tetraindole core structure, making the system more susceptible to oxidation (*p*-doping) rather than reduction (*n*-doping).

The anodic CVs of arylated cyclooctatetraindoles are depicted in Figure 3b. All these compounds exhibited overlapped

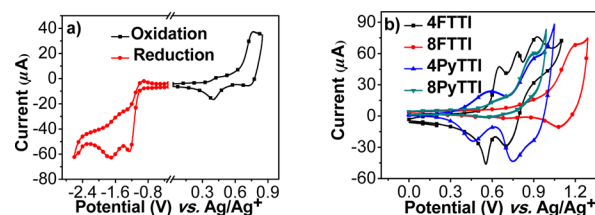


Figure 3. CV curves of cyclooctatetraindoles in films.

multireversible oxidation waves, attributed to the oxidation of the cyclic tetraindole core and the aryl substituents. The onset of the oxidation potentials was found to be 0.50, 0.70, 0.32, and 0.47 V, respectively, corresponding to HOMO values in the range of -5.03 to -5.41 eV. The LUMO levels were deduced from the HOMO and optical band gaps ranging from -2.32 to -2.93 eV (Table S2).

In summary, we have applied a facile and simple one-pot synthetic procedure for the first direct synthesis of C_{2v} -symmetric cyclic tetraindole with an 8π annulene as the center. A cyclocondensation mechanism has been proposed for the formation of cyclic tri- and tetraindole via treatment of indolin-2-one with POCl_3 . Based on the core structure, a novel series of tetra- and octa-arylated tetraindole derivatives with fluorene and pyrene substituents have thus been readily constructed. The thermal, optical, and electrochemical properties were investigated to understand the role of the tetraindole core structure on functional properties of the resultant molecules. The results showed unique optoelectronic characteristics with wide optical band gaps and redox-active properties. The interesting structural and electronic properties of the novel symmetric cyclic tetraindole with an 8π annulene as the center reported herein hold promise for potential applications of tetraindole-based materials in the field of molecular electronics. Further study in this direction is ongoing.

■ ASSOCIATED CONTENT

Supporting Information

General experimental procedures, NMR, MALDI-TOF-MS, and detailed description of experiments. These materials are available free of charge via the Internet at <http://pubs.acs.org>.

■ AUTHOR INFORMATION

Corresponding Authors

*E-mail: iamwylai@njupt.edu.cn.

*E-mail: iamwhuang@njupt.edu.cn.

Author Contributions

[§]These authors contributed equally.

Notes

The authors declare no competing financial interest.

■ ACKNOWLEDGMENTS

We acknowledge financial support from the National Key Basic Research Program of China (973 Program, 2014CB648300, 2009CB930601), the National Natural Science Foundation of China (20904024, 51173081, 61136003, 61106036), the Natural Science Foundation of Jiangsu Province (BK20130037, BK2011760), Program for New Century Excellent Talents in University (NCET-13-0872), Specialized Research Fund for the Doctoral Program of Higher Education (20133223110008), the Ministry of Education of China (IRT1148), the NUPT Scientific Foundation (NY213119, NY210016), the Priority Academic Program Development of Jiangsu Higher Education Institutions (PAPD), the Six Talent Plan (2012XCL035), and the Qing Lan Project of Jiangsu Province. We are grateful to Weidong Xu and Xiaochun Fan at IAM for the experimental and characterization assistance.

■ REFERENCES

- (1) (a) Sundberg, R. J. *The Chemistry of Indoles*; Academic Press: New York, 1996. (b) Kochanowska-Karamyan, A. J.; Hamann, M. T. *Chem. Rev.* **2010**, *110*, 4489.
- (2) Berkes, B. B.; Inzelt, G. *Electrochim. Acta* **2014**, *122*, 11.
- (3) (a) Janosik, T.; Wahlström, N.; Bergman, J. *Tetrahedron* **2008**, *64*, 9159. (b) Wakim, S.; Bouchard, J.; Simard, M.; Drolet, N.; Tao, Y.; Leclerc, M. *Chem. Mater.* **2004**, *16*, 4386. (c) Wu, Y.; Li, Y.; Gadner, S.; Ong, B. S. *J. Am. Chem. Soc.* **2005**, *127*, 614.
- (4) Wang, E.; Mammo, W.; Andersson, M. R. *Adv. Mater.* **2014**, *26*, 1801.
- (5) (a) Lai, W. Y.; Zhu, R.; Fan, Q. L.; Hou, L. T.; Cao, Y.; Huang, W. *Macromolecules* **2006**, *39*, 3707. (b) Lai, W. Y.; Chen, Q. Q.; He, Q. Y.; Fan, Q. L.; Huang, W. *Chem. Commun.* **2006**, *18*, 1959. (c) Lai, W. Y.; He, Q. Y.; Zhu, R.; Chen, Q. Q.; Huang, W. *Adv. Funct. Mater.* **2008**, *18*, 265. (d) Lai, W. Y.; Liu, D.; Huang, W. *Science China Chem.* **2010**, *53*, 2472. (e) Lai, W. Y.; He, Q. Y.; Chen, D. Y.; Huang, W. *Chem. Lett.* **2008**, *37*, 986. (f) Feng, G. L.; Lai, W. Y.; Ji, S. J.; Huang, W. *Tetrahedron Lett.* **2006**, *47*, 7089. (g) Levermore, P. A.; Xia, R.; Lai, W. Y.; Wang, X. H.; Huang, W.; Bradley, D. D. C. *J. Phys. D: Appl. Phys.* **2007**, *40*, 1896. (h) Zhu, R.; Lai, W. Y.; Wang, H. Y.; Yu, N.; Wei, W.; Peng, B.; Huang, W.; Hou, L. T.; Peng, J. B.; Cao, Y. *Appl. Phys. Lett.* **2007**, *90*, 141909.
- (6) (a) Lu, Z.; Li, C.; Fang, T.; Li, G.; Bo, Z. *J. Mater. Chem. A* **2013**, *1*, 7657. (b) Qian, X.; Zhu, Y. Z.; Song, J.; Gao, X. P.; Zheng, J. Y. *Org. Lett.* **2013**, *15*, 6034.
- (7) (a) Garcia-Frutos, E. M.; Omenat, A.; Barbera, J.; Serrano, J. L.; Gomez-Lor, B. *J. Mater. Chem.* **2011**, *21*, 6831. (b) Gallego-Gómez, F.; Garcia-Frutos, E. M.; Villalvilla, J. M.; Quintana, J. A.; Gutierrez-Puebla, E.; Monge, A.; Díaz-García, M. A.; Gómez-Lor, B. *Adv. Funct. Mater.* **2011**, *21*, 738. (c) Zhao, B.; Liu, B.; Peng, R. Q.; Zhang, K.; Lim, K. A.; Luo, J.; Shao, J.; Ho, P. K. H.; Chi, C.; Wu, J. *Chem. Mater.* **2010**, *22*, 435.
- (8) (a) Franceschin, M.; Ginnari-Satriani, L.; Alvino, A.; Ortaggi, G.; Bianco, A. *Eur. J. Org. Chem.* **2010**, *134*. (b) Capelli, L.; Manini, P.; Pezzella, A.; d'Ischia, M. *Org. Biomol. Chem.* **2010**, *8*, 4243.
- (9) (a) Harpham, M. R.; Süzer, Ö.; Ma, C.-Q.; Bäuerle, P.; Goodson, T., III. *J. Am. Chem. Soc.* **2009**, *131*, 973. (b) Miyasaka, M.; Pink, M.; Rajca, S.; Rajca, A. *Angew. Chem., Int. Ed.* **2009**, *48*, 5954.
- (10) (a) Matsuura, A.; Komatsu, K. *J. Am. Chem. Soc.* **2001**, *123*, 1768. (b) Lu, P.; Hong, H.; Cai, G.; Djurovich, P.; Weber, W. P.; Thompson, M. E. *J. Am. Chem. Soc.* **2000**, *122*, 7480.
- (11) (a) Nishiuchi, T.; Tanaka, K.; Kuwatani, Y.; Sung, J.; Nishinaga, T.; Kim, D.; Iyoda, M. *Chem.—Eur. J.* **2013**, *19*, 4110. (b) Nishinaga, T.; Ohmae, T.; Aita, K.; Takase, M.; Iyoda, M.; Araib, T.; Kunugi, Y. *Chem. Commun.* **2013**, *49*, 5354. (c) Lin, F.; Peng, H. Y.; Chen, J. X.; Chik, D. T. W.; Cai, Z. W.; Wong, K. M. C.; Yam, V. W. W.; Wong, H. N. C. *J. Am. Chem. Soc.* **2010**, *132*, 16383. (d) Lai, C. W.; Lam, C. K.; Lee, H. K.; Mak, T. C. W.; Wong, H. N. C. *Org. Lett.* **2003**, *5*, 823. (e) Mouri, K.; Saito, S.; Yamaguchi, S. *Angew. Chem., Int. Ed.* **2012**, *51*, 5971.
- (12) Heinz, W.; Räder, H.-J.; Müllen, K. *Tetrahedron Lett.* **1989**, *30*, 159.
- (13) (a) Marsella, M. J.; Reid, R. J. *Macromolecules* **1999**, *32*, 5982. (b) Marsella, M. J.; Reid, R. J.; Estassi, S.; Wang, L. S. *J. Am. Chem. Soc.* **2002**, *124*, 12507.
- (14) Sygula, A.; Fronczek, F. R.; Sygula, R.; Rabideau, P. W.; Olmstead, M. M. *J. Am. Chem. Soc.* **2007**, *129*, 3842.
- (15) Nishiuchi, T.; Kuwatani, Y.; Nishinaga, T.; Iyoda, M. *Chem.—Eur. J.* **2009**, *15*, 6838.
- (16) See computational calculations about a symmetric indole tetramer: Yurtsever, M.; Yurtsever, E. *Polymer* **2002**, *43*, 6019.
- (17) Talaz, O.; Saracoglu, N. *Tetrahedron* **2010**, *66*, 1902.
- (18) Hiyoshi, H.; Sonoda, T.; Mataka, S. *Heterocycles* **2006**, *68*, 763.
- (19) (a) Lai, W. Y.; Xia, R.; Bradley, D. D. C.; Huang, W. *Chem.—Eur. J.* **2010**, *16*, 8471. (b) Lai, W. Y.; Liu, D.; Huang, W. *Macromol. Chem. Phys.* **2011**, *212*, 445.